



CHORUS

This is the accepted manuscript made available via CHORUS. The article has been published as:

Optical tunneling by arbitrary macroscopic three-dimensional objects

Lei Bi, Ping Yang, George W. Kattawar, and Michael I. Mishchenko

Phys. Rev. A **92**, 013814 — Published 8 July 2015

DOI: [10.1103/PhysRevA.92.013814](https://doi.org/10.1103/PhysRevA.92.013814)

Optical Tunneling by Arbitrary Macroscopic 3D Objects

Lei Bi,¹ Ping Yang,^{1,2,*} George W. Kattawar,² and Michael I. Mishchenko³

¹*Department of Atmospheric Sciences, Texas A&M University, College Station, Texas, 77843*

²*Department of Physics and Astronomy, Texas A&M University, College Station, Texas, 77843*

³*NASA Goddard Institute for Space Studies, New York, New York, 10025*

(Dated: May 21, 2015)

Electromagnetic wavefront portions grazing or nearly grazing the surface of a macroscopic particle contribute to the extinction of the incident radiation through a tunneling process similar to the scenario of barrier penetration in quantum mechanics. The aforesaid tunneling contribution, referred to as the edge effect, is critical to a correct depiction of the physical mechanism of electromagnetic extinction. Although an analytical solution for the edge effect in the case of a sphere has been reported in the literature, the counterparts for non-spherical particles remain unknown. The conventional curvature-based formalism of the edge effect breaks down in the case of faceted particles. As the first success, this paper reports a novel method, based on the invariant imbedding principle and the Debye expansion technique, to accurately quantify the edge effect associated with an arbitrarily shaped three-dimensional object. The present method also provides a rigorous capability to facilitate the validation of various empirical approximations for electromagnetic extinction. Canonical results are presented to illustrate optical tunneling for two non-spherical geometries.

PACS numbers: 42.68.Mj, 92.60.Ta

Keywords: Extinction, Tunneling, Edge Effect

I. INTRODUCTION

Diffraction in classical macroscopic electrodynamics exhibits a tunneling effect similar to that in quantum mechanics [1, 2]. As an incident wave strikes a particle, the interaction between the particle and the wavefront portions that graze or nearly graze the obstacle's edges leads to tunneling composed of the above-edge and below-edge components according to the localization principle [3]. The above-edge effect is due to localized waves that are beyond the particle's cross section and propagate in the surrounding medium without being scattered by the particle, whereas the below-edge effect is related to anomalous reflection that gives rise to additional forward scattering [3]. Because electromagnetic tunneling occurs near the edges of particles, the tunneling efficiency is traditionally referred to as the edge effect or the edge phenomenon [3]. To date, rigorous studies of the edge effect have been limited to spheres and infinite circular cylinders [3–6]. It would be a significant leap towards a better understanding of electromagnetic extinction if the edge effect could be accurately quantified in the case of non-spherical particles. Furthermore, the solution for the optical tunneling associated with an arbitrarily shaped particle is extremely valuable from practical application perspective, as most natural particles of interest are non-spherical (e.g., hexagonal ice crystals in the atmosphere and spheroids as approximations to the overall shapes of many particles in nature [7–9]).

It is unlikely feasible to derive an analytical solution for the edge effect associated with a general non-spherical particle from Maxwell's equations. Classical approaches

to studying the edge effect are based on Fock's principle of the local field for a conducting or nearly conducting particle with smoothly varying curvature [10]. Pioneering work by Nussenzweig and Wiscombe [5] in the case of a dielectric sphere was based on the Debye expansion of the Lorenz-Mie series [11, 12]. An innovative application of the complex angular momentum theory to the Debye series [5] yields an approximate formula for the edge-effect contribution to the extinction efficiency of a homogeneous sphere and demonstrates that the edge effect for a sphere is associated with the forward scattering amplitude of the zeroth-order Debye series. The Debye approach has been extended to spheroids and layered spherical particles [13] based on the method of separation of variables, and to more general homogeneous non-spherical shapes based on the extended boundary condition method [14]. However, in the previous studies, numerical instability and nonconvergence issues limited the efforts to small size parameters, and thus the relationship between the edge effect and the zeroth-order Debye series has not been revealed. To understand the edge effect, the solution to the Debye diffraction and reflection must be obtained in the semi-classical domain where the localization principle is approximately valid.

This paper reports a novel method based on the invariant imbedding principle to obtain the Debye diffraction and reflection. The tunneling efficiency is computed from the forward scattering amplitude from the optical theorem [3]. The invariant imbedding concept is an outgrowth of the principle of invariance introduced by Ambarzumyan [15] to solve atmospheric radiative transfer, and the firm foundations of the aforesaid concept were developed by a late Nobel laureate, S. Chandrasekhar [16]. The present novel method can be applied to arbitrary non-spherical particles for the edge-effect solution

* pyang@tamu.edu

in a size-parameter range where the ray concept is applicable. To the best of the authors' knowledge, reported in this paper is the first success in accurately quantifying the edge effect for non-spherical particles, which has important implications for many practical applications [7].

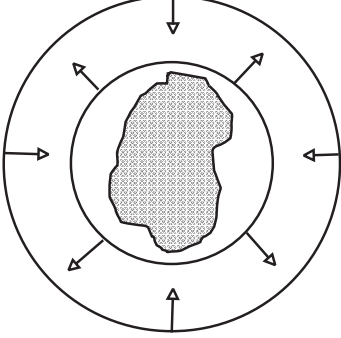


FIG. 1. Reflection of an incoming spherical wave by a non-spherical particle.

II. METHOD

Figure 1 illustrates the reflection of an incoming spherical wave to outgoing spherical waves by a non-spherical particle. In terms of Debye's diffraction and reflection, the incident wave is an incoming spherical wave,

$$\mathbf{E}^{inc}(\mathbf{r}) = \sum_{l=1}^{\infty} \tilde{a}_l \tilde{\mathbf{M}}_l(kr) + \tilde{b}_l \tilde{\mathbf{N}}_l(kr), \quad (1)$$

and the reflected wave is given by

$$\mathbf{E}^{ref}(\mathbf{r}) = \sum_{l=1}^{\infty} \tilde{p}_l \mathbf{M}_l(kr) + \tilde{q}_l \mathbf{N}_l(kr). \quad (2)$$

In Eqs. (1) and (2), \mathbf{M} and \mathbf{N} are vector spherical wave functions constructed from spherical Hankel functions of the first kind, and $\tilde{\mathbf{M}}$ and $\tilde{\mathbf{N}}$ are similar to \mathbf{M} and \mathbf{N} except that spherical Hankel functions of the first kind are replaced with the second kind; k is the wave number defined as $k = 2\pi/\lambda$ in which λ is the incident wavelength. Note $l = n(n+1) + m$ is an index defined to combine

the angular momentum number n and the projected angular momentum number m . The reflection matrix can be symbolically defined as

$$\begin{bmatrix} \tilde{p} \\ \tilde{q} \end{bmatrix} = \mathbf{R} \begin{bmatrix} \tilde{a} \\ \tilde{b} \end{bmatrix}. \quad (3)$$

With Eq.(1) expanded in terms of regular vector spherical wave functions and Eq.(2) defined as the total scattered field, the matrix relating the coefficients is referred to as the T-matrix [8], which contains the total extinction efficiency, and can be expanded into the Debye series [14]. To compute the edge effect contribution to the extinction efficiency, the following zeroth-order T-matrix is defined

$$\mathbf{T}^0 = -\frac{1}{2}(\mathbf{1} - \mathbf{R}), \quad (4)$$

from which the extinction efficiency of a randomly oriented particle can be given as the sum of 2 (owing to the Fraunhofer diffraction and the blocking of the incident light) and the edge effect contribution in the form

$$\begin{aligned} Q_{ext} &= 2 + Q_{edge} \\ &= -\frac{2\pi}{k^2 \langle S \rangle} \text{Re} \sum_{l=1}^{l_{max}} [T_{ll}^{0,11} + T_{ll}^{0,22}], \end{aligned} \quad (5)$$

where $\langle S \rangle$ is the average projected-area of the scattering particle. For a particle with a fixed orientation, the edge-effect efficiency can be obtained from the amplitude scattering matrix in the forward scattering direction, given by \mathbf{T}^0 via a process similar to obtaining the total extinction efficiency from \mathbf{T} [8, 17, 18]. Furthermore, we found that \mathbf{T}^0 satisfies the following matrix Riccati differential equation,

$$\begin{aligned} \frac{d\mathbf{T}^0(kr)}{d(kr)} &= i \left[\mathbf{J}^T(kr) + \mathbf{T}^0(kr) \mathbf{H}(kr) \mathbf{J}^T(kr) \right] \\ &\quad \times \mathbf{U}(kr) \left[\mathbf{J}(kr) + \mathbf{H}(kr) \mathbf{T}^0(kr) \right]. \end{aligned} \quad (6)$$

In Eq.(6), $\mathbf{T}^0(kr)$ indicates the zeroth-order T-matrix of a partial volume of the particle within a sphere of radius r , \mathbf{J} is the real part of \mathbf{H} , and \mathbf{H} and \mathbf{U} are super matrices with each element given by

$$H_{ll'} = \delta_{ll'} \begin{bmatrix} h_n^{(1)}(kr) & 0 \\ 0 & \frac{1}{kr} \frac{\partial}{\partial r} [r h_n^{(1)}(kr)] \\ 0 & \sqrt{n(n+1)} h_n^{(1)}(kr) / kr \end{bmatrix}, \quad (7)$$

$$\begin{aligned} U_{ll'} &= k^2 r^2 (-1)^{m+m'} \left[\frac{2n+1}{4\pi n(n+1)} \right]^{1/2} \left[\frac{2n'+1}{4\pi n'(n'+1)} \right]^{1/2} \int_0^{2\pi} d\phi \int_0^\pi d\theta \sin\theta \exp[-i(m-m')\phi] [\epsilon(r, \theta, \phi) - 1] \\ &\quad \times \begin{bmatrix} \pi_{mn}(\theta) \pi'_{mn}(\theta) + \tau_{mn}(\theta) \tau_{mn'}(\theta) & -i[\pi_{mn}(\theta) \tau'_{mn}(\theta) + \tau_{mn}(\theta) \pi_{mn'}(\theta)] & 0 \\ i\pi_{mn}(\theta) \tau'_{mn}(\theta) + i\tau_{mn}(\theta) \pi_{mn'}(\theta) & \pi_{mn}(\theta) \pi'_{mn}(\theta) + \tau_{mn}(\theta) \tau_{mn'}(\theta) & 0 \\ 0 & 0 & \tilde{d}_{0m}^n(\theta) \tilde{d}_{0m'}^{n'}(\theta) / \tilde{n}^2 \end{bmatrix}, \end{aligned} \quad (8)$$

where $h_n^{(1)}(kr)$ is a spherical Hankel function of the first kind, $\pi_{mn}(\theta) = m/\sin\theta d_{0m}^n(\theta)$, $\tau_{mn}(\theta) = d/d\theta d_{0m}^n(\theta)$ and $\tilde{d}_{0m}^n = \sqrt{n(n+1)}d_{0m}^n$ with d_{0m}^n being the Wigner-d function; \tilde{m} is the complex refractive index and ϵ is permittivity and equal to \tilde{m}^2 . Given the initial value, the solution of $\mathbf{T}^0(kr)$ can be numerically obtained. Note that for a non-spherical particle, the initial value can be selected to be \mathbf{T}^0 associated with the inscribed sphere, whose reflection matrix is diagonal, namely,

$$R_{ll'} = \delta_{ll'} \begin{bmatrix} R_{nn}^{11} & 0 \\ 0 & R_{nn}^{22} \end{bmatrix}. \quad (9)$$

The diagonal elements in Eq.(9) can be obtained from the method of separation of variables and appropriate wave boundary conditions on the spherical particle surface, given by (e.g., see [19])

$$R_{nn}^{11} = \frac{\zeta_n^{(2)'}(x)\zeta_n^{(2)}(\tilde{m}x) - \tilde{m}\zeta_n^{(2)}(x)\zeta_n^{(2)'}(\tilde{m}x)}{-\zeta_n^{(1)'}(x)\zeta_n^{(2)}(\tilde{m}x) + \tilde{m}\zeta_n^{(1)}(x)\zeta_n^{(2)'}(\tilde{m}x)}, \quad (10)$$

$$R_{nn}^{22} = \frac{\tilde{m}\zeta_n^{(2)'}(x)\zeta_n^{(2)}(\tilde{m}x) - \zeta_n^{(2)}(x)\zeta_n^{(2)'}(\tilde{m}x)}{-\tilde{m}\zeta_n^{(1)'}(x)\zeta_n^{(2)}(\tilde{m}x) + \zeta_n^{(1)}(x)\zeta_n^{(2)'}(\tilde{m}x)}, \quad (11)$$

where $x = kr_s$ is the size parameter (r_s is the sphere radius), and $\zeta_l^{(i)}(x)$ is the Riccati-Bessel function defined with spherical Hankel function of the i th kind. We employ the classic 4th order Runge-Kutta method for the numerical solution of Eq. (6). A mathematical proof of the fundamental relation in Eq.(6) is provided in Appendix A and the validation in the case of a sphere is given in Appendix B.

III. RESULTS

The present numerical method can be readily employed to examine Fock's principle of the local field [10]. According to Fock, the edge effect is a consequence of the local characteristics of an object in the penumbra region and involves the curvature and impedance. It means that two different particle shapes with the same local characteristics have the same edge-effect efficiency. To test this conjecture, we consider a scattering problem with the incident light striking a sphere or an incomplete sphere, as shown in Fig. 2. The direction of the incident light is along the symmetry axis of the incomplete sphere. The total extinction efficiencies for the two particles are different if the particle is non-absorptive or weakly absorptive; however, the edge efficiencies for the two geometries should be the same, if the edge effect is solely associated with the local characteristics of geometry. Figure 2 shows the comparison of the edge-effect efficiencies of the two geometries in a wide size-parameter range for three different refractive indices. The ratio of the diameter to the height of the incomplete sphere is 1.2. The agreement of the numerical results affirms Fock's principle of the local field for a dielectric particle with a curved boundary that separates the illuminated and shadow sides.

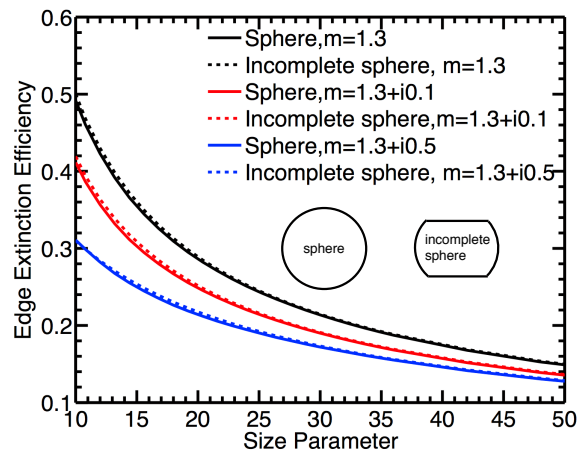


FIG. 2. Comparison of the edge extinction efficiencies for a sphere and an incomplete sphere as functions of the size parameter.

Figure 3 shows a comparison of the extinction efficiencies of spheroids with the end-on incidence computed from different approaches to affirm the edge-effect contribution to the total extinction efficiency. Rigorous total extinction efficiencies are computed from the T-matrix method [18]. The dotted lines are calculated from the zeroth-order Debye series as the sum of 2 and the edge-effect contribution. Circles are computed from the addition of the rigorous solution of the edge effect and approximate geometric-optics results. Similar to a spherical particle, the geometric-optics contribution of the forward amplitude scattering matrix is only from the central ray and can be modified from the formula of the spherical case [5] with a divergence factor correction. The extinction efficiency formula containing the physics of Fraunhofer diffraction and the central ray transmission is given in Eq. (19) of Bi and Yang [21].

In the upper panel, the particle is moderately absorptive, thus the higher-order transmission must be considered in the computation of the extinction efficiency. As the particle size increases, the edge-effect efficiency decreases. As evident, the summation of the edge effect and geometric-optics term closely agree with the exact solution of the total extinction efficiency. In the lower panel, the particle is highly absorptive, and the transmission can be reasonably neglected. Therefore, the total extinction efficiency arises primarily from the Debye reflection and diffraction, which contains the Fraunhofer diffraction, the geometric-optics reflection (blocking effect), and the edge effect.

In addition to particles of smoothly varying curvature, the present numerical method can be applied to faceted particles without technical restrictions. Figure 4 shows the edge-effect contribution for randomly oriented hexagonal ice crystals. We found the edge effect to be significant when the particle is non-absorptive or weakly absorptive and quite small for highly absorptive particles.

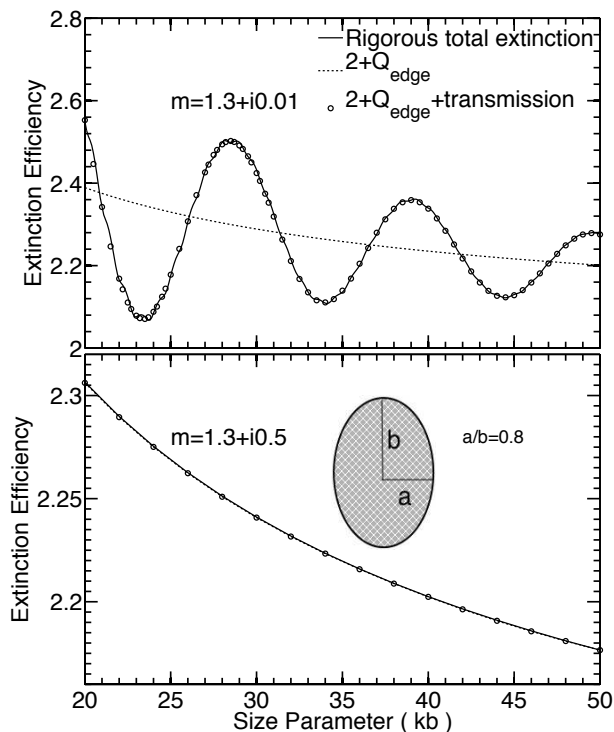


FIG. 3. Extinction efficiencies of spheroids with the end-on incidence. Upper panel: the refractive index is $1.3+i0.01$; Lower panel is similar to Upper panel except that the refractive index is $1.3+i0.5$.

In comparison to spheres and spheroids, the edge-effect efficiencies for hexagonal particles are generally small. The edge-effect efficiency's dependence on the size parameter is similar to that of spheres or spheroids.

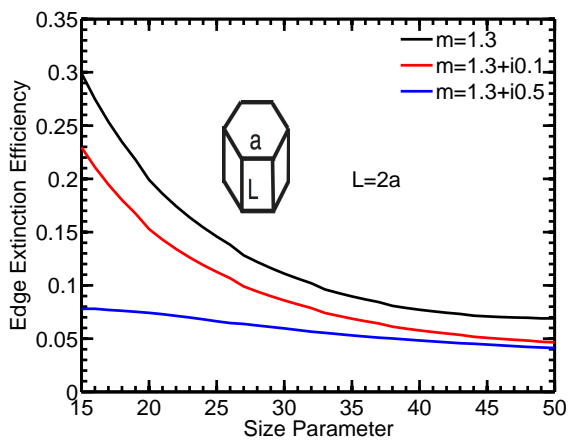


FIG. 4. Comparison of the edge-effect efficiencies of hexagonal particles for three refractive indices.

To obtain the semi-empirical formula of the edge effect for convex conducting particles with smoothly varying

curvature, Jones [22] derived an edge-effect term based on the assumption that near a glancing point the obstacle behaves like a cylinder with its axis tangent to the curve of glancing points. Jones' approach is developed within the framework of Fock's principle of local field. Based on Jones' rationale and Nussenzveig's results of the extinction efficiency obtained from the complex angular momentum theory, the semi-empirical calculations for the edge effect in the dielectric spheroid case have been reported in Bi and Yang [21]. Note that Jones' approximate method for the edge-effect calculations relies on the radius of curvature of the boundary separating the illuminated and the shadow sides. However, the relationship between the radius of curvature and the edge-effect efficiency is not applicable to faceted particles. If Jones' rationale is applied to a faceted particle, the edge-effect contribution could be incorrectly infinite.

To understand the physical reasons that decrease the edge-effect efficiency, we therefore surmise that the below-edge effect substantially decreases because the interference between the forward reflection and diffraction may not exist. To test this assumption, the above-edge effect for axially symmetric particles with the incident light aligned with the symmetry axis can be separated from the total edge effect based on the localization principle [3], given by

$$Q_{edge,abv} = \frac{-2}{(ka)^2} \text{Re} \left[\sum_{n=1}^{\infty} (2n+1) \sum_{n'=n_0}^{\infty} \sqrt{\frac{2n'+1}{2n+1}} i^{n'-n} \left(T_{1n1n'}^{0,11} + T_{1n1n'}^{0,12} + T_{1n1n'}^{0,21} + T_{1n1n'}^{0,22} \right) \right] \quad (12)$$

where $n_0 = [ka - 1/2]$ is associated with the grazing rays ($[\cdot]$ indicates the integer part of the argument.). Then, the below-edge effect efficiency is given by

$$Q_{edge,bel} = Q_{edge} - Q_{edge,abv} \quad (13)$$

We compared the edge-effect efficiencies for particles by modifying the particle boundaries (Fig. 5) and found the edge effect to be dominated by the above-edge effect if the below-edge boundary is faceted, which annihilates the forward reflection. As an example, for $m=1.3$, $ka=20.5$, and $kb=15$, the total edge-effect efficiency is 0.1023, the above-edge efficiency is 0.0883 and the below-edge efficiency is 0.014.

IV. CONCLUSION

We have demonstrated that the edge effect contribution to the extinction efficiency can be rigorously quantified from first principles by solving the zeroth-order Debye series. The conventional curvature-based depiction of the edge effect for particles with curved surfaces is directly validated in the case of spheroids, but the curvature-based edge-efficiency formalism breaks down

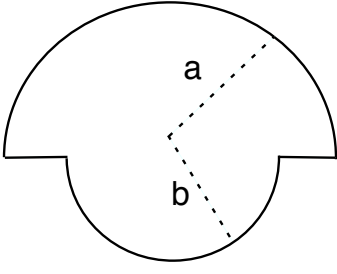


FIG. 5. A schematic geometry to annihilate the interference between the forward reflection and the diffraction.

in the case of faceted particles. However, from the perspective of practical applications of the edge effect with reasonably accurate numerical solution, an approximate formula of the edge effect can be obtained by parameterizing the numerical results. As illustrated by the present results, the tunneling effect strongly depends on the scattering particle's geometric configuration. The significance of this study is that, as the first success, a feasible approach is developed to determine the edge effect associated with general non-spherical particles.

ACKNOWLEDGMENTS

This study was supported by an NSF grant (AGS-1338440) and an NASA grant (NNX11AK37G). PY and MIM acknowledge support from the NASA Remote Sensing Theory program.

Appendix A: Proof of Eq. (6)

We derive Eq. (6) from an electric field volume integral equation and validate the results in the case of a sphere. The electric field volume integral equation reads [8]

$$\bar{E}(r) = \bar{E}^{inc}(r) + k^2 \int [\tilde{m}(r')^2 - 1] \bar{G}(r - r') \bar{E}(r') d^3 r' \quad (\text{A1})$$

where $\bar{E}^{inc}(r)$ is the incident electric field, $\bar{E}(r)$ is the total electric field, and $\bar{G}(r - r')$ is the dyadic Green's function. Note that in Eq. (A1) and all following equations, a variable with a single bar represents a three-component column vector in the spherical coordinate system and a variable with double bar represents a matrix. The derivation of Eq. (6) is similar to that employed in deriving the invariant imbedding T-matrix equation [17] except for the representation of the source field and the expansion of the dyadic Green's function with respect to vector spherical wave functions. To treat the singularity problem, the total electric field in source free regions \bar{E}^{eff} is

defined. Eq. (A1) is written as [17]

$$\bar{E}^{eff}(r) = \bar{E}^{inc}(r) - \int \bar{G}(r - r') u(r') \bar{Z}(r') \bar{E}^{eff}(r') d^3 r', \quad (\text{A2})$$

where $u(r') = [\tilde{m}(r')^2 - 1]$ and $\bar{Z} = (1/\tilde{m}^2) \hat{r} \hat{r} + \hat{\theta} \hat{\theta} + \hat{\phi} \hat{\phi}$. To obtain the direct external reflection of an incoming spherical wave, dyadic Green's function is expanded as

$$\bar{G}(r, r') = \frac{1}{2} \sum_{n=1}^{\infty} \sum_{m=-n}^n \bar{Y}_{mn}(\theta, \phi) \bar{g}_n(r, r') \bar{Y}_{mn}^+(\theta', \phi') \quad (\text{A3})$$

where

$$\bar{Y}_{mn}(\theta, \phi) = (-1)^m \left[\frac{2n+1}{4\pi n(n+1)} \right] \exp(im\phi) \times \begin{bmatrix} 0 & 0 & \sqrt{n(n+1)} d_{0m}^n(\theta) \\ i\pi_{mn}(\theta) & \tau_{mn}(\theta) & 0 \\ -\tau_{mn}(\theta) & i\pi_{mn}(\theta) & 0 \end{bmatrix} \quad (\text{A4})$$

and

$$\bar{g}_n(r, r') = \begin{cases} ik \bar{H}_n(r) \bar{H}_n^+(r'); & r > r' \\ \frac{ik}{2} [\bar{H}_n(r) \bar{H}_n^+(r') + \bar{H}_n^*(r) \bar{H}_n^T(r')]; & r = r' \\ ik \bar{H}_n^*(r) \bar{H}_n^T(r'); & r < r' \end{cases} \quad (\text{A5})$$

Realizing that the incoming spherical wave is represented as $\bar{Y}_{mn}(\theta, \phi) \bar{H}_n^*(r) = (\bar{\mathbf{M}}_{mn}(kr), \bar{\mathbf{N}}_{mn}(kr))$, Eq. (A2) is written as

$$\bar{E}_{m'n'}(r) = \bar{Y}_{m'n'}(\theta, \phi) \bar{H}_{n'}^*(r) + \int_0^{r_m} dr' \sum_{n=1}^{\infty} \sum_{m=-n}^n \bar{Y}_{mn}(\theta, \phi) \bar{g}_n(r, r') \bar{F}_{mnm'n'}(r'), \quad (\text{A6})$$

where

$$\bar{F}_{mnm'n'}(r) = \frac{r^2}{2} \int d\Omega \bar{Y}_{mn}^+(\theta, \phi) u(r) \bar{Z}(r) \bar{E}_{m'n'}(r). \quad (\text{A7})$$

Substituting Eq. (A6) in Eq. (A7), we have

$$\begin{aligned} \bar{F}_{mnm'n'}(r) &= \bar{V}_{mnm'n'}(r) \bar{H}_{n'}^*(r) \\ &+ \sum_{\underline{n}=\underline{m}=-\underline{n}}^{\infty} \sum_{\underline{m}=-\underline{n}}^{\underline{n}} \bar{V}_{mnm\underline{m}\underline{n}}(r) \\ &\times \int_0^{r_m} dr' \bar{g}_{\underline{n}}(r, r') \bar{F}_{\underline{m}\underline{m}'\underline{n}'}(r'), \end{aligned} \quad (\text{A8})$$

where \bar{V} is given by

$$\bar{V}_{mnm'n'}(r) = \frac{r^2}{2} \int d\Omega \bar{Y}_{mn}^+(\theta, \phi) u(r) \bar{Z}(r) \bar{Y}_{m'n'}(\theta, \phi) \quad (\text{A9})$$

Note that $\bar{V} = \bar{U}/2$, where 2 is from the Wronskian identity. Let $r > r'$. Then, the integral term in Eq. (A6) is the reflection field. The \bar{R} matrix can be written as

$$\bar{R}_{mnm'n'}(r_m) = ik \int_0^{r_m} dr' \bar{H}_n^+(r') \bar{F}_{mnm'n'}(r') \quad (\text{A10})$$

To numerically compute the \bar{R} matrix, the definite integral of Eq. (A10) is approximated as a weighted sum of function values at specific points in the domain of integration,

$$\bar{R}(r_s) = ik \sum_{j=1}^s w_j \bar{H}^+(r_j) \bar{F}(r_s|r_j), \quad (\text{A11})$$

where w_j is weight, s is the total number of division points, and $\bar{F}(s|r_j)$ is the solution of

$$\begin{aligned} \bar{F}(r_s|r_j) &= \bar{V}(r_j) \bar{H}^*(r_j) \\ &+ \bar{V}(r_j) \sum_{i=1}^s w_i \bar{g}(r_j, r_i) \bar{F}(r_s|r_i). \end{aligned} \quad (\text{A12})$$

Once the linear equations of Eq. (A12) are solved, \bar{R} can be readily computed through summation. The concept of the invariant imbedding approach is to compute $\bar{R}(r_s)$ based on $\bar{R}(r_{s-1})$ without solving Eq. (A12). Let the upper limit in the integral of $\bar{R}(r)$ (Eq. (A10)) be r_{s-1} , we have

$$\bar{R}(r_{s-1}) = ik \sum_{j=1}^{s-1} w_j \bar{H}^+(r_j) \bar{F}(r_{s-1}|r_j) \quad (\text{A13})$$

and

$$\begin{aligned} \bar{F}(r_{s-1}|r_j) &= \bar{V}(r_j) \bar{H}^*(r_j) \\ &+ \bar{V}(r_j) \sum_{i=1}^{s-1} w_i \bar{g}(r_j, r_i) \bar{F}(r_{s-1}|r_i). \end{aligned} \quad (\text{A14})$$

The relationship between $\bar{F}(r_s|r_j)$ and $\bar{F}(r_{s-1}|r_j)$ can be found from the equation,

$$L[\text{A12}] \times R[\text{A14}] - R[\text{A12}] \times L[\text{A14}] = 0, \quad (\text{A15})$$

which gives

$$\begin{aligned} &\bar{V}(r_j) \sum_{i=1}^{s-1} w_i \bar{g}(r_j, r_i) \\ &\times \left[\bar{F}(r_s|r_j) \bar{F}(r_{s-1}|r_i) - \bar{F}(r_{s-1}|r_j) \bar{F}(r_s|r_i) \right] \\ &+ \bar{V}(r_j) \left\{ \bar{H}^*(r_j) \left[\frac{\bar{F}(r_s|r_j)}{\bar{F}(r_{s-1}|r_j)} - 1 \right] \right. \\ &\left. - w_s \bar{g}(r_j, r_s) \bar{F}(r_s|r_s) \right\} \bar{F}(r_{s-1}|r_j) = 0. \end{aligned} \quad (\text{A16})$$

L and R in Eq. (A15) mean the left- and right-hand sides of the involved equation. Dropping $\bar{V}(r_j)$, taking summation $\sum_{j=1}^{s-1}$, and noting that

$$\begin{aligned} &\sum_{j=1}^{s-1} \sum_{i=1}^{s-1} w_i \bar{g}(r_j, r_i) \\ &\times \left[\bar{F}(r_s|r_j) \bar{F}(r_{s-1}|r_i) - \bar{F}(r_{s-1}|r_j) \bar{F}(r_s|r_i) \right] = 0 \end{aligned} \quad (\text{A17})$$

we obtain

$$\begin{aligned} &\sum_{j=1}^{s-1} \left\{ H^*(r_j) \left[\frac{F(r_s|r_j)}{F(r_{s-1}|r_j)} - 1 \right] \right. \\ &\left. - w_s g(r_j, r_s) F(r_s|r_s) \right\} F(r_{s-1}|r_j) = 0. \end{aligned} \quad (\text{A18})$$

Because Eq. (A18) is valid for any scattering systems, all the coefficients of $F(r_{s-1}|r_j)$ should be zero, namely,

$$H^*(r_j) \left[\frac{\bar{F}(r_s|r_j)}{\bar{F}(r_{s-1}|r_j)} - 1 \right] = ik w_s g(r_j, r_s) F(r_s|r_s) \quad (\text{A19})$$

Using Eq. (A5) with $r_j < r_s$, we have

$$\frac{\bar{F}(r_s|r_j)}{\bar{F}(r_{s-1}|r_j)} = 1 + ik w_s \bar{H}^T(r_s) \bar{F}(r_s|r_s), \quad (\text{A20})$$

which is independent of r_j . To relate $\bar{R}(r_s)$ and $\bar{R}(r_{s-1})$, we define

$$\bar{q}(r_s) = ik \sum_{j=1}^{s-1} w_j \bar{H}^+(r_j) \bar{F}(r_s|r_j). \quad (\text{A21})$$

Then, we have

$$\bar{q}(r_s) = \bar{R}(r_{s-1}) \left[1 + ik w_s \bar{H}^T(r_s) \bar{F}(r_s|r_s) \right] \quad (\text{A22})$$

$$= \bar{R}(r_s) - ik w_s \bar{H}^+(r_s) \bar{F}(r_s|r_s). \quad (\text{A23})$$

Another relation between $\bar{F}(r_s|r_s)$ and $\bar{q}(r_s)$ can be obtained from Eq. (A12). Let $r_j = r_s$ in Eq. (A12), we obtain

$$\begin{aligned} \bar{F}(r_s|r_s) &= \bar{V}(r_s) \bar{H}^*(r_s) \\ &+ \bar{V}(r_s) \sum_{i=1}^{s-1} w_i \bar{g}(r_s, r_i) \bar{F}(r_s|r_i) \\ &+ w_s \bar{V}(r_s) \bar{g}(r_s, r_s) \bar{F}(r_s|r_s). \end{aligned} \quad (\text{A24})$$

Solving the preceding equation in terms of $\bar{F}(r_s|r_s)$ gives

$$\begin{aligned} \bar{F}(r_s|r_s) &= w_s^{-1} w_s \frac{\bar{V}(r_s)}{1 - w_s \bar{V}(r_s) \bar{g}(r_s, r_s)} \\ &\times \left[\bar{H}^*(r_s) + \bar{H}(r_s) \bar{q}(r_s) \right]. \end{aligned} \quad (\text{A25})$$

Define

$$\bar{Q}(r_s) = \frac{w_s \bar{V}(r_s)}{1 - w_s \bar{V}(r_s) \bar{g}(r_s, r_s)}. \quad (\text{A26})$$

Then,

$$\bar{F}(r_s|r_s) = w_s^{-1} \bar{Q}(r_s) \left[\bar{H}^*(r_s) + \bar{H}(r_s) \bar{q}(r_s) \right]. \quad (\text{A27})$$

Substituting Eq. (A27) into Eq. (A22) yields

$$\bar{q}(r_s) = \bar{R}(r_{s-1}) \left\{ 1 + \left[\bar{Q}_{21}(r_s) + \bar{Q}_{22}(r_s) \bar{q}(r_s) \right] \right\} \quad (\text{A28})$$

where

$$\bar{Q}_{21}(r_s) = ik\bar{H}^T(r_s)\bar{Q}(r_s)\bar{H}^*(r_s), \quad (\text{A29})$$

$$\bar{Q}_{22}(r_s) = ik\bar{H}^T(r_s)\bar{Q}(r_s)\bar{H}(r_s). \quad (\text{A30})$$

Solving Eq. (A28) in terms of $\bar{q}(r_s)$ gives

$$\bar{q}(r_s) = [1 - \bar{R}(r_{s-1})\bar{Q}_{2,2}(r_s)]^{-1}\bar{R}(r_{s-1}) \left[1 + \bar{Q}_{2,1}(r_s) \right] \bar{q}(r_{s-1}) \quad (\text{A31})$$

From Eq. (A23)

$$\bar{R}(r_s) = \bar{Q}_{11}(r_s) + \left[1 + \bar{Q}_{12}(r_s) \right] \bar{q}(r_s), \quad (\text{A32})$$

where

$$\bar{Q}_{11}(r_s) = ik\bar{H}^+(r_s)\bar{Q}(r_s)\bar{H}^*(r_s), \quad (\text{A33})$$

$$\bar{Q}_{12}(r_s) = ik\bar{H}^+(r_s)\bar{Q}(r_s)\bar{H}(r_s). \quad (\text{A34})$$

Therefore

$$\begin{aligned} \bar{R}(r_s) &= \bar{Q}_{11}(r_s) + \left[1 + \bar{Q}_{12}(r_s) \right] \\ &\times \left[1 - \bar{R}(r_{s-1})\bar{Q}_{2,2}(r_s) \right]^{-1} \bar{R}(r_{s-1}) \\ &\times \left[1 + \bar{Q}_{2,1}(r_s) \right]. \end{aligned} \quad (\text{A35})$$

Formally, Eq. (A35) can be employed to compute the reflection matrix of the particle by growing the particle in a layer-by-layer form. From Eqs. (A22) and (A23), we have,

$$\begin{aligned} \frac{\bar{R}(r_s) - \bar{R}(r_{s-1})}{w_s} &= ik \left[\bar{H}^+(r_s) + \bar{R}(r_{s-1})\bar{H}^T(r_s) \right] \\ &\times \bar{F}(r_s|r_s). \end{aligned} \quad (\text{A36})$$

Letting $w_s \rightarrow 0$, we obtain

$$\bar{F}(r_s|r_s) = \bar{V}(r_s) \left[\bar{H}^*(r_s) + \bar{H}(r_s)\bar{R}(r_s) \right], \quad (\text{A37})$$

because

$$w_s^{-1}\bar{Q}(r_s) = \bar{V}(r_s), \quad (\text{A38})$$

$$\bar{q}(r_s) = \bar{R}(r_s). \quad (\text{A39})$$

Substituting Eq. (A37) into Eq. (A36) gives

$$\begin{aligned} \frac{d\bar{R}(kr)}{d(kr)} &= \frac{i}{2} \left[\bar{H}^+(kr) + \bar{R}(kr)\bar{H}^T(kr) \right] \\ &\bar{U}(kr) \left[\bar{H}^*(kr) + \bar{H}(kr)\bar{R}(kr) \right], \end{aligned} \quad (\text{A40})$$

By letting $\bar{T} = -1/2(1 - \bar{R})$, we have Eq. (6).

Similar to the T-matrix computation [18], Eq. (A35) provides a natural procedure to compute the reflection matrix. Unfortunately, the numerical implementation requires fairly small step sizes to avoid the ill-conditioning problem in the computation of the Q matrix. When the order of Bessel function n is much greater than

$x + 4.02x^{1/3}$, the $g_n(x, x)$ matrix has fairly large eigenvalues. Mathematically, the step size w should be sufficiently small so that the geometric series

$$\frac{1}{1 - w\bar{V}(x)\bar{g}(x, x)} \quad (\text{A41})$$

converge (such numerical difficulty is nonexistent in the computation of T-matrix). Therefore, numerical implementation based on Eq. (A35) is only applicable to solving the reflection matrix of nearly spherical particles.

In this study, we solve first-order ordinary differential equations of Riccati type Eq. (6) by using the 4th order Runge-Kutta method. Although it becomes challenging to apply Eq. (6) to large aspect ratios or large particle sizes due to the stiffness problem, we can obtain accurate solutions for a range of size parameters, where the edge effect is pronounced.

The preceding discussions are limited to homogeneous particles. In the case of particles with inclusions, the edge effect is solely dependent on the refractive index of the host particle. A direct confirmation of this statement from the invariant imbedding method is not straightforward, because the derivative of the reflection matrix is discontinuous (e.g., for a coated sphere). However, for an inhomogeneous sphere with a continuous variation of the refractive index in the radial direction, we found the result to be the same as that of a homogeneous particle with the refractive index of the outermost layer of the inhomogeneous sphere.

Appendix B: Sphere

In the case of a sphere, the \bar{U} matrix is given as follows,

$$\bar{U}_{mnm'n'}(r) = k^2 r^2 (\tilde{m}^2 - 1) \delta_{mm'} \delta_{nn'} \begin{bmatrix} 1 & 0 & 0 \\ 0 & 1 & 0 \\ 0 & 0 & 1/\tilde{m}^2 \end{bmatrix} \quad (\text{B1})$$

Substituting Eq. (B1) into Eq. (A36), we have

$$\begin{aligned} \frac{dR_{nn}^{11}(kr)}{d(kr)} &= i \frac{\tilde{m}^2 - 1}{2} \left[R_{nn}^{11}(kr) \zeta_n^{(1)}(kr) + \zeta_n^{(2)}(kr) \right]^2 \quad (\text{B2}) \\ \frac{dR_{nn}^{22}(kr)}{d(kr)} &= i \frac{\tilde{m}^2 - 1}{2} \left\{ \left[\frac{n(n+1)}{\tilde{m}^2(kr)^2} \right], \right. \\ &\times \left[R_{nn}^{22}(kr) \zeta_n^{(1)}(kr) + \zeta_n^{(2)}(kr) \right]^2 \\ &\left. + \left[R_{nn}^{22}(kr) \zeta_n^{(1)}(kr) + \zeta_n^{(2)}(kr) \right]^2 \right\}. \end{aligned} \quad (\text{B3})$$

This section shows the derivation of Eqs. (B2) and (B3) from Eqs. (10) and (11) as a direct validation of the results obtained from the previous section. For simplicity in taking derivatives of the reflection matrix, we define

$$A(x) = \zeta_n^{(2)'}(x) \zeta_n^{(2)}(\tilde{m}x) - \tilde{m} \zeta_n^{(2)}(x) \zeta_n^{(2)'}(\tilde{m}x), \quad (\text{B4})$$

$$B(x) = -\zeta_n^{(1)'}(x) \zeta_n^{(2)}(\tilde{m}x) + \tilde{m} \zeta_n^{(1)}(x) \zeta_n^{(2)'}(\tilde{m}x), \quad (\text{B5})$$

$$U(x) = \tilde{m} \zeta_n^{(2)'}(x) \zeta_n^{(2)}(\tilde{m}x) - \zeta_n^{(2)}(x) \zeta_n^{(2)'}(\tilde{m}x), \quad (\text{B6})$$

$$D(x) = -\tilde{m} \zeta_n^{(1)'}(x) \zeta_n^{(2)}(\tilde{m}x) + \zeta_n^{(1)}(x) \zeta_n^{(2)'}(\tilde{m}x), \quad (\text{B7})$$

such that

$$R_{nn}^{11}(x) = \frac{A(x)}{B(x)}, \quad (\text{B8})$$

$$R_{nn}^{22}(x) = \frac{U(x)}{D(x)}. \quad (\text{B9})$$

By employing the Wronskian identity

$$\zeta_n^{(2)}(x)\zeta_n^{(1)'}(x) - \zeta_n^{(2)'}(x)\zeta_n^{(1)}(x) = 2i, \quad (\text{B10})$$

we obtain from Eq. (B4) and Eq. (B5)

$$A(x)\zeta_n^{(1)}(x) + B(x)\zeta_n^{(2)}(x) = -2i\zeta_n^{(2)}(\tilde{m}x), \quad (\text{B11})$$

$$A(x)\zeta_n^{(1)'}(x) + B(x)\zeta_n^{(2)'}(x) = -2i\tilde{m}\zeta_n^{(2)'}(\tilde{m}x). \quad (\text{B12})$$

The derivative of Eq. (B11) in terms of x minus Eq. (B12) yields

$$A'(x)\zeta_n^{(1)}(x) + B'(x)\zeta_n^{(2)}(x) = 0. \quad (\text{B13})$$

Taking Eq.(B11) $\times A'(x)$ –Eq.(B13) $\times A(x)$, we have

$$\begin{aligned} A'(x)B(x) - A(x)B'(x) &= \frac{A'(x)}{\zeta_n^{(2)}(x)} \left[-2i\zeta_n^{(2)}(\tilde{m}x) \right] \\ &= -2i \left[\frac{\zeta_n^{(2)''}(x)}{\zeta_n^{(2)}(x)} \zeta_n^{(2)}(\tilde{m}x) - \tilde{m}^2 \zeta_n^{(2)''}(\tilde{m}x) \right] \zeta_n^{(2)}(\tilde{m}x). \end{aligned} \quad (\text{B14})$$

By using the identity

$$\tilde{m}^2 \zeta_n''(\tilde{m}x) + \left[\tilde{m}^2 - \frac{n(n+1)}{x^2} \right] \zeta_n(\tilde{m}x) = 0, \quad (\text{B15})$$

or, equivalently,

$$\frac{\zeta_n''(\tilde{m}x)}{\zeta_n(\tilde{m}x)} = \left[\frac{n(n+1)}{(\tilde{m}x)^2} - 1 \right]. \quad (\text{B16})$$

Eq. (B14) is simplified to

$$A'(x)B(x) - A(x)B'(x) = -2i(\tilde{m}^2 - 1) \left[\zeta_n^{(2)}(\tilde{m}x) \right]^2 \quad (\text{B17})$$

From Eq. (B8) and Eq. (B17), we have

$$\frac{dR_{nn}^{11}(x)}{dx} = -2i(\tilde{m}^2 - 1) \left[\frac{\zeta_n^{(2)}(\tilde{m}x)}{B(x)} \right]^2. \quad (\text{B18})$$

Using Eq. (B11) and Eq. (B8), the preceding equation can be written as

$$\frac{dR_{nn}^{11}(x)}{dx} = \frac{i}{2}(\tilde{m}^2 - 1) \left[R_{nn}^{11}(x)\zeta_n^{(1)}(x) + \zeta_n^{(2)}(x) \right]^2 \quad (\text{B19})$$

Similarly, applying Eq. (B10) to Eq. (B6) and Eq. (B7) gives

$$U(x)\zeta_n^{(1)}(x) + D(x)\zeta_n^{(2)}(x) = -2i\tilde{m}\zeta_n^{(2)}(\tilde{m}x), \quad (\text{B20})$$

$$U(x)\zeta_n^{(1)'}(x) + D(x)\zeta_n^{(2)'}(x) = -2i\zeta_n^{(2)'}(\tilde{m}x). \quad (\text{B21})$$

The derivative of Eq. (B20) minus Eq. (B21) leads to

$$\begin{aligned} U'(x)\zeta_n^{(1)}(x) + D'(x)\zeta_n^{(2)}(x) \\ = -2i(\tilde{m}^2 - 1)\zeta_n^{(2)'}(\tilde{m}x). \end{aligned} \quad (\text{B22})$$

Taking Eq.(B20) $\times U'(x)$ –Eq.(B22) $\times U(x)$, we have

$$\begin{aligned} U'(x)D(x) - U(x)D'(x) \\ = \frac{2i \left[-\tilde{m}\zeta_n^{(2)}(\tilde{m}x)U'(x) + (\tilde{m}^2 - 1)\zeta_n^{(2)'}(\tilde{m}x)U(x) \right]}{\zeta_n^{(2)}(x)} \\ = 2i\tilde{m}^2 \left(\frac{\zeta_n^{(2)''}(y)}{\zeta_n^{(2)}(\tilde{m}x)} - \frac{\zeta_n^{(2)''}(x)}{\zeta_n^{(2)}(x)} \right) \left[\zeta_n^{(2)}(\tilde{m}x) \right]^2 \\ - 2i(\tilde{m}^2 - 1) \left[\zeta_n^{(2)'}(\tilde{m}x) \right]^2 \\ = 2i(\tilde{m}^2 - 1) \left\{ \frac{n(n+1)}{x^2} \left[\zeta_n^{(2)}(\tilde{m}x) \right]^2 - \left[\zeta_n^{(2)'}(\tilde{m}x) \right]^2 \right\}. \end{aligned} \quad (\text{B23})$$

The derivative of Eq. (B9) can be written as

$$\begin{aligned} \frac{dR_{nn}^{22}(x)}{dx} &= 2i(\tilde{m}^2 - 1) \\ &\times \left\{ \frac{n(n+1)}{x^2} \left[\frac{\zeta_n^{(2)}(\tilde{m}x)}{D(x)} \right]^2 - \left[\frac{\zeta_n^{(2)'}(\tilde{m}x)}{D(x)} \right]^2 \right\} \\ &= -\frac{i}{2}(\tilde{m}^2 - 1) \left\{ \frac{n(n+1)}{(\tilde{m}x)^2} \right. \\ &\times \left[R_{nn}^{22}\zeta_n^{(1)}(x) + \zeta_n^{(2)}(x) \right]^2 \\ &\left. - \left[R_{nn}^{22}\zeta_n^{(1)'}(x) + \zeta_n^{(2)'}(x) \right]^2 \right\}. \end{aligned} \quad (\text{B24})$$

In Eq. (B24), we have used Eqs. (B9), (B20) and (B21). Note that the reflection coefficients given by Eqs. (10) and (11) are obtained from the method of separation of variables and appropriate boundary conditions. Thus, Eq. (A40) in the case of a sphere is validated.

-
- [1] H. M. Nussenzveig and W. J. Wiscombe, Phys. Rev. Lett. 59, 1667 (1987).
[2] H. M. Nussenzveig, Prog. Opt. 50, 185 (2007).
[3] H. C. van de Hulst, *Light Scattering by Small particles* (Dover, 1981).
[4] T. T. Wu, Phys. Rev. 104, 1201 (1956).

- [5] H. M. Nussenzveig and W. J. Wiscombe, Phys. Rev. Lett. 45, 1490 (1980).
[6] W. T. Grandy, *Scattering of Waves from Large Spheres* (Cambridge University, 2000).
[7] M. I. Mishchenko, J. W. Hovenier, and L. D. Travis, eds., *Light Scattering by Nonspherical Particles: Theory, Mea-*

- surements, and Applications* (Academic, 1999).
- [8] M. I. Mishchenko, *Electromagnetic Scattering by Particles and Particle Groups: An Introduction* (Cambridge, 2014).
- [9] P. Chylek and J. D. Klett, *J. Opt. Soc. Am. A* 8, 274 (1991).
- [10] V. A. Fock, *Electromagnetic Diffraction and Propagation Problems* (Pergamon, 1965).
- [11] P. Debye, *Phys. Zeit.* 9, 775 (1908).
- [12] B. Van de Pol and H. Bremmer, *Phil. Mag.* 24, 141, 823 (1937).
- [13] J. A. Lock, J. M. Jamison, and C.-Y. Lin, *Appl. Opt.* 33, 4677 (1994).
- [14] F. Xu, J. A. Lock, and G. Gouesbet, *Phys. Rev. A* 81, 043824 (2010).
- [15] V. A. Ambarzumyan, *C. R. Acad. Sci. SSSR* , 38, 229 (1943).
- [16] S. Chandrasekhar, *Radiative Transfer* (Dover, 1960).
- [17] B. R. Johnson, *App. Opt.* 27, 4861 (1988).
- [18] L. Bi and P. Yang, *J. Quant. Spectrosc. Radiat. Transfer.* 138, 17 (2014).
- [19] E. A. Hovenac and J. A. Lock, *J. Opt. Soc. Am. A* 9, 781 (1992).
- [20] See Supplemental Material at ...
- [21] L. Bi and P. Yang, *Opt. Express*, 22, 10270 (2014).
- [22] D. S. Jones, *Proc. R. Soc. Lond. A Math. Phys. Sci.* 240, 206 (1957).